Microswimmer-driven agglutination assay

Diana Isabel Sandoval Bojórquez

Thesis submitted for the degree of
Erasmus Mundus Master of Science
in Nanoscience and Nanotechnology,
specialization in Biophysics.

TU Dresden Promoters:
Prof. Gianaurelio Cuniberti
Prof. Hans-Georg Braun

KU Leuven Co-Promoter:
Prof. Christiaan Van Hoof

Academic Year: 2018-2019

Erasmus Mundus Master in Nanoscience and Nanotechnology

Biotechnology Center

Erasmus Mundus Master in Nanoscience and Nanotechnology

Microswimmer-driven agglutination assay

A Thesis

By

Diana Isabel Sandoval Bojórquez

Submitted in partial fulfillment of the requirements

for the degree of

Master of Science

First Assessor: Professor Gianaurelio Cuniberti

Second Assessor: Professor Hans-Georg Braun

KU Leuven Supervisor: Professor Christiaan Van Hoof

Date of submission: August 5th, 2019.

Abstract

Lab-on-a-chip systems for point-of-care testing demonstrate a promising development towards more accurate diagnostic tests that are of extreme importance for the future global health. This work presents an agglutination assay performed in micrometer sized well using Janus PS/Ag/AgCl micromotors to enhance the interactions between goat anti-human IgM functionalized particles and Human IgM. The fabricated microwell chips are a suitable platform to analyze the interaction between different particles and to perform the agglutination assays. The interaction between active Janus particles and passive and functionalized particles is studied, as well as the influence of ions on the motion of the Janus particles. Agglutination assays are performed with and without the presence of Janus particles, and in different PBS concentrations. Once illuminated with blue light, passive SiO_2 particles were effectively excluded from Janus particles, while SiO_2–NH_2 particles revealed attraction. In contrast, functionalized SiO_2–NH_2-Ab particles suspended in PBS did not show any interaction. It was found that the optimal working conditions for antibodies and Janus particles differed and, as a result, the Janus particles did not reveal a desirable interaction between the functionalized particles and IgM. Further experiments should be performed to find the proper conditions in which the antibodies and the Janus particles maintain their activities. It is believed that an effective interaction between the functionalized and Janus particles could be achieved by modifying the parameters that affect their interaction such as the zeta potential and the medium in which the assay is being performed. This preliminary work provides the first steps towards the development of a fully-integrated lab-on-a-chip system for point-of-care testing.

Acknowledgments

I would like to express my gratitude to Dr. Larysa Baraban for allowing me to participate in this project. I would particularly like to thank Tao Huang who taught me all the techniques required to realize this work, thank you for your time and your patience. Thanks to the BioNanoSensorics group for the very helpful advice and the very interesting lunch talks.

I would like to sincerely thank Prof. Gianaurelio Cuniberti, Prof. Hans-Georg Braun and Prof. Christiaan Van Hoof for agreeing to be the promoters of this work, for their valuable feedback, and their time.

I would like to thank the European Commission for granting me the scholarship that allowed me to realize these master studies. I feel extremely grateful for their support, without it, I would not have been able to follow this program.

Sergio, thank you for taking this journey with me. Your love, support, and kindness made this adventure an extraordinary experience.

Finally, I would like to thank my family, especially my parents. Thank you for all your love, support and the long phone talks. Thanks for believing in me.

Table of Contents

List of Tables

List of Figures

Abbreviations

A.U.	Arbitrary units
BSA	Bovine serum albumin
C	Capacity of the particle surface for a given antibody
DI	Deionized
DLA	Diffusion limited aggregation
fps	Frames per second
LFIA	Lateral flow immunoassays
LOC	Lab-on-a-chip
PBS	Phosphate buffered saline
PEG	Poly(ethylene glycol)
POC	Point-of-care
PS	Polystyrene
PVP	Polyvinylpyrrolidone
rpm	Revolutions per minute
SEM	Scanning electron microscope

1. Introduction

Medical diagnosis is a key aspect of human health care. It attempts to determine the cause of the symptoms experienced by a person by means of an evaluation of the patient's history and a physical examination[1]. However, considering that most of the symptoms are not specific to particular disease, other procedures such as diagnostic tests should be performed to discern between diseases or conditions that produce very similar behaviors. Therefore, the use of diagnostic tests has become an essential element of the medical diagnosis process[2].

1.1 In vitro diagnostic tests

In vitro diagnostic tests are one of the most used tests in assisting the medical diagnosis process[3,4]. This type of tests examine specimens from the human body such as blood, serum, saliva, urine and tissue[3–5]. Since in vitro diagnostics is fundamental for early detection, monitoring the stages of a disease, and accurate prognosis, there is a need to develop more accurate tests that at the same time can fulfill the requirements of global health[6].

The challenges of the development of diagnostic tests arise from the fact that diseases can be originated by different factors such as specific gene mutations or infections caused by parasites, bacteria or viruses[7–10]. In addition, the time for each disease to manifest symptoms can vary since, at early stages, the amount of bacteria or virus is not enough to produce an immune response[9].

Another important constrain to the design of diagnostic tests is that the access to health care facilities in which many of these tests are performed are not available for all the people in need of them. This can be due to the scarcity of specialized laboratories or to the elevated costs[11]. For that reason, it is important to develop diagnostic tests that do not need specialized equipment and that can be performed at the place of patient care[2].

1.1.1 Point-of-care tests

Point-of-care (POC) tests refer to tests that can be performed near or at the place where the patient is[2,12]. The idea of POC test is that they should be able to be used by the patient itself, this implies that the test should require minimum sample preparation, fast response, digital or visible readout and user-friendly equipment[6]. All these characteristics make POC tests very attractive since they would allow rapid clinical decision making, better disease monitoring, decrease costs, and allow them to be employed in places where there is no adequate infrastructure[2,6,12].

Lateral flow immunoassays (LFIA) are one of the most popular POC tests[6,13]. Their technical basis is derived from the latex agglutination assay first realized by Plotz and Singer in 1956[14]. Among the LFIA, the pregnancy dipstick tests are the most widely used[6]. A typical LFIA strip and the operation of LFIA are shown in Figure 1.

The principle of the LFIA is the following: a liquid sample is applied on an absorbent pad and moves through the test strip by capillary action interacting with molecules present in the test strip[13]. If the sample contains the analyte of interest it will interact with antibodies that are present in the conjugate release pad. These antibodies are conjugated to colored or fluorescent particles. The analyte of interest bounded to the conjugated antibodies will further migrate to the detection zone in which specific antigens or antibodies are immobilized. These will react with the analyte bound to conjugated antibodies. If there is recognition of the analyte of interest a colored test line will appear. However, a control line would always appear and it indicates a proper liquid flow through the test strip[6,13].

1.2 Agglutination assay

Agglutination of cells or particles refers to the formation of clumps by the interaction of specific antibodies against the respective antigens present in the surface of the cells or the particles[15]. This reaction can be used to detect the presence of antibodies in human sera and body fluids[15,16]. Different antigens such as pathogens, bacteria, fungi, and viruses can also be detected[15,17].

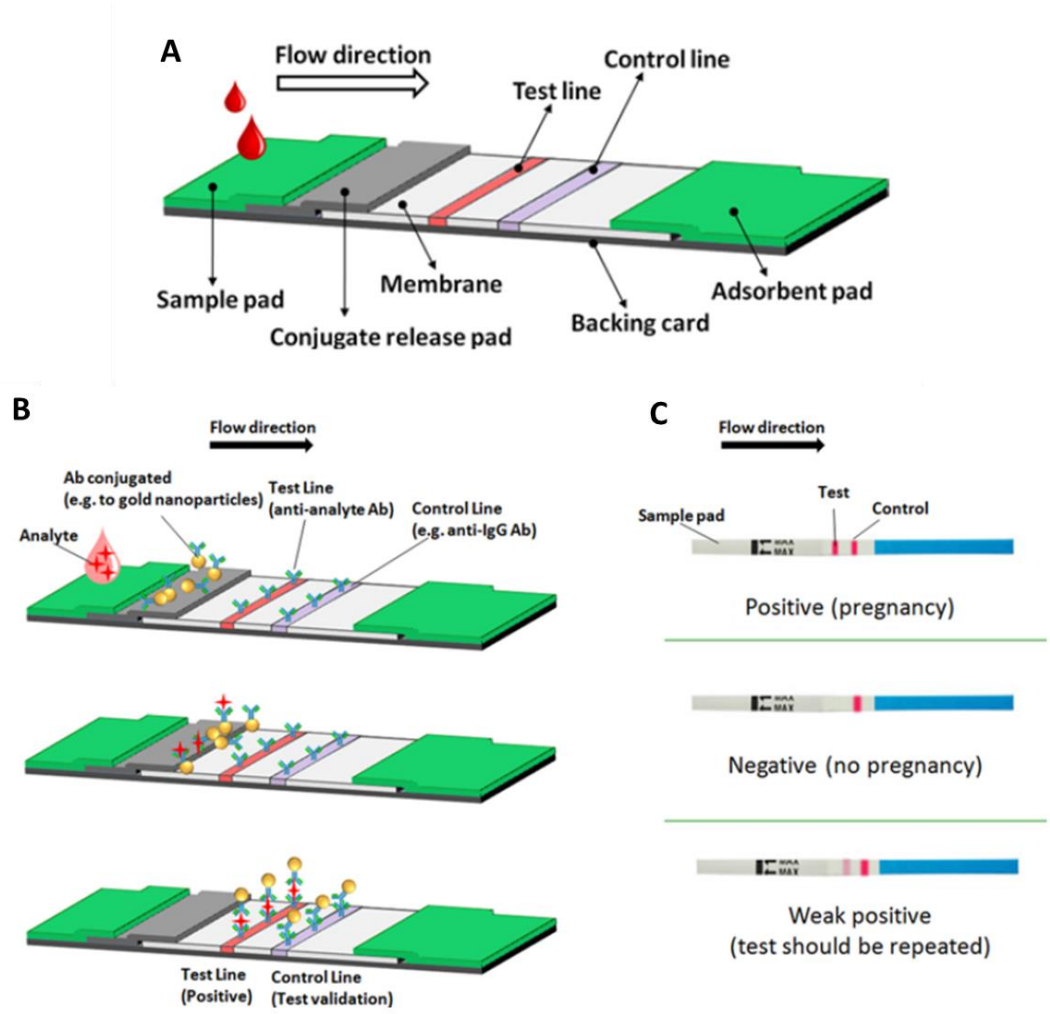

Figure 1. Lateral flow immunoassay. (A) Configuration of a lateral flow immunoassay test strip. (B) Schematic representation of the operation of the assay. Top: sample is deposited on the sample pad and migrates to the conjugated antibodies. Middle: the conjugated antibodies bind to the analyte. Bottom: migration of the bound target analyte to the test line where it is captured. (C) Pregnancy test (One Step hCG Urine Test) possible results and interpretation. Image adapted from Koczula and Gallotta[13].

Antigens form large agglomerates when the specific antibodies are present as a result of the several recognition sites that antibodies have[16]. These agglomerates are visible without magnification; however, to improve visualization, antibodies can be attached to the surface of latex particles. This assay is known as indirect agglutination assay or latex agglutination assay since the agglutination of the particles will be the indicator of the presence of the antigen in solution[14,17]. The latex agglutination assay can be used to detect either antigens or antibodies since the particles can be functionalized at convenience as it is presented in Figure 2.

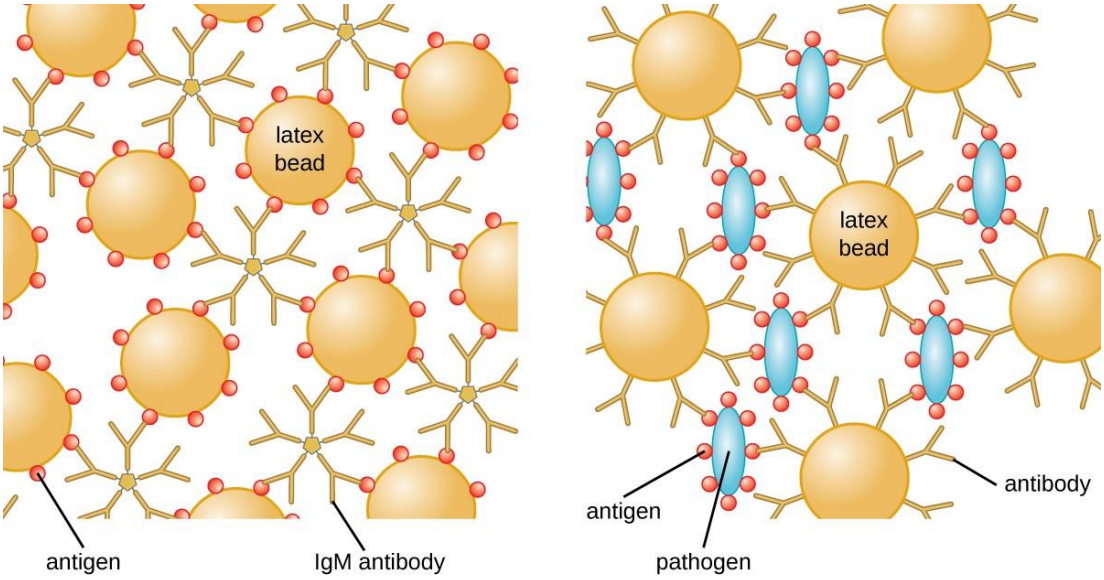

Figure 2. Indirect agglutination assay. (A) Possitive agglutination test for antibodies and (B) possitive agglutination test for antigens[18].

Latex agglutination assays have been employed to detect different diseases such as rheumatoid arthritis, HIV, dengue, typhoid fever, and bladder tumors[14,15,19–21]. Some of the advantages of using this technique for diagnosis are the increased efficiency of antigen-antibody binding due to a large surface area compared to ELISA, decrease in assay time as a result of a high surface to volume ratio (increase reaction rate), and the possibility to perform the assay using different types of samples[17]. On the other hand, some of the disadvantages that latex agglutination tests have are that sample preparation is required and the results are qualitative and semi-quantitative[15].

Overall, latex agglutination assays are of great interest to be implemented as POC tests since the equipment required to perform the assay is minimal compared to other techniques such as ELISA[15,17]. The use technologies such as lab-on-a-chip and biosensors could eliminate the sample preparation steps and give more accurate and quantitative results[22,23].

1.3 Lab-on-a-chip

The term lab-on-a-chip (LOC) is attributed to the miniaturization of one or more laboratory techniques into a small chip of up to few square centimeters in size[24]. Laboratory work at this scale is appealing since the time, reagents and waste are reduced[25]. The compact integration of the components such as biosensors and microfluidic elements, and the short analysis and response time due to shorter diffusion distances that can be achieve with LOC technology make them an important ally to the development of POC tests[22]. Figure 3 shows an example of the integration of several analytical techniques to develop a LOC system for POC testing.

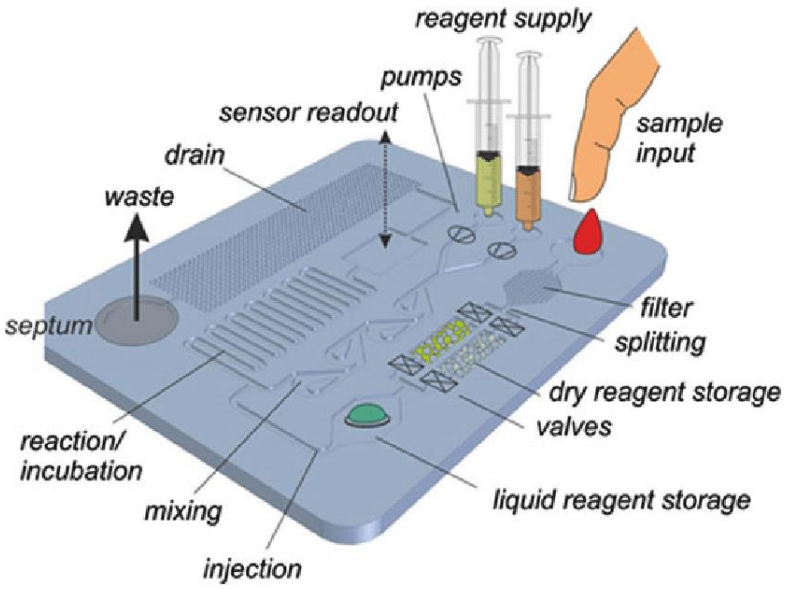

Figure 3. Lab-on-a-chip device for point-of-care testing[26].

Recent trends have suggested the integration of nanomaterials to LOC technology to improve the sensitivity and selectivity of the analytical operations due to the interesting surface properties that nanomaterials can exhibit[25]. Additionally, smart materials such as micro- and nanomotors that move by different propulsion mechanisms can perform interesting tasks such as cargo transport and induce the collective behavior of particles[27–29]. These characteristics can add different and more complex functionalities to the LOC technology.

1.4 Self-propelled particles

Self-propelled particles, also known as microswimmers and micromotors, are microscale devices that have been especially designed to exhibit motion as a response to specific stimuli[30]. Their development was triggered by Feynman's visionary talk in 1959 in which he introduced the idea of small machines that could move and perform complex tasks[31].

Figure 4 shows some examples of microswimmers using different propulsion mechanisms. Bubble propulsion is one of the most studies mechanisms and it involves the decomposition of a fuel by a catalyst which results in the formation of gas bubbles leading to rocket-like propulsion[32]. Ultrasound can be used as an external stimulus to propel asymmetric particles since this asymmetry will induce the generation of pressure gradients that would lead them to move unidirectionally[32]. Rotary external magnetic fields can propel magnetic helix by transforming the rotation around their axis into translational corkscrew motion[33]. Light can also be used as an external stimulus since it can induce phoretic self-propulsion by means of a photocatalytic reaction[34].

Microswimmers have demonstrated their functionalities in different applications such as cargo transport, environmental remediation, sensing, drug delivery, and imaging[35]. For each of these applications, microswimmers should meet certain requirements such as the use of biocompatible materials for biomedical applications. Of special interest are light-driven microswimmers since they have a fuel-free propulsion mechanism and have shown to act collectively and also induce collective behavior in other particles around them. These characteristics make them appealing for applications such as the transport and deliver of cargo[28].

1.4.1 Light-driven Ag/AgCl micromotors

Wang et al., have reported the collective behavior of passive polystyrene (PS) beads induced by blue-light-actuated PS/Ag/AgCl Janus micromotors in pure water[29]. The plasmonic Ag/AgCl cap of the Janus micromotors enables them to absorb blue light which generates the photodecomposition of silver chloride as shown in Equation 1.

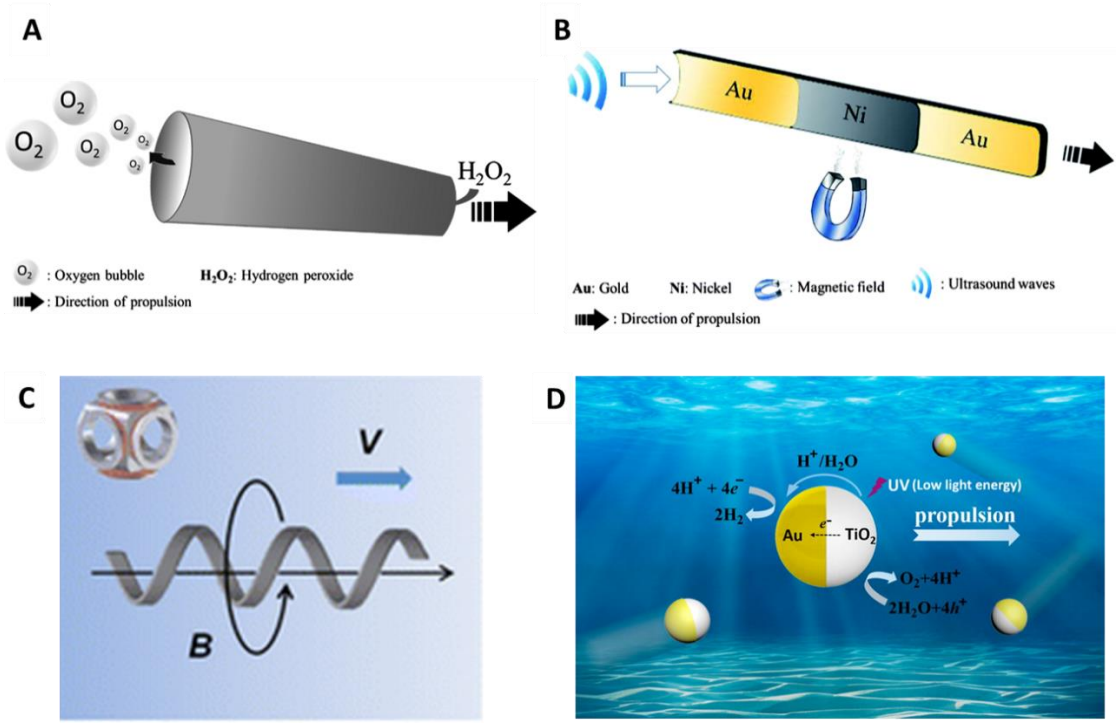

Figure 4. Microswimmmers and their different propulsion mechanisms. (A) Schematic representation of a microswimmer propelled by bubbles[32]. (B) Schematic representation of an Au-Ni-Au nanowire propelled by ultrasound and guided by an external magnetic field[32]. (C) Schematic representation of the corkscrew motion of a magnetic helix in the presence of a rotating magnetic field[33]. (D) Schematic representation of the motion of Janus particles by light-induced phoretic self-propulsion[34].

$$4\,AgCl + 2H_2O \xrightarrow{hv,\ Ag^+} 4\,Ag + 4\,H^+ + 4\,Cl^- + O_2 \qquad (1)$$

This reaction is illustrated in Figure 5A. As a result of the photodecomposition of silver chloride, a local chemical gradient is self-generated and thus the Janus microswimmers move due to self-diffusiophoresis[36]. The mechanism of self-diffusiophoresis is illustrated in Figure 5B, where it is visible that the generated ions diffuse at different rates, leading to a net electric field pointing towards the Janus cap[37].

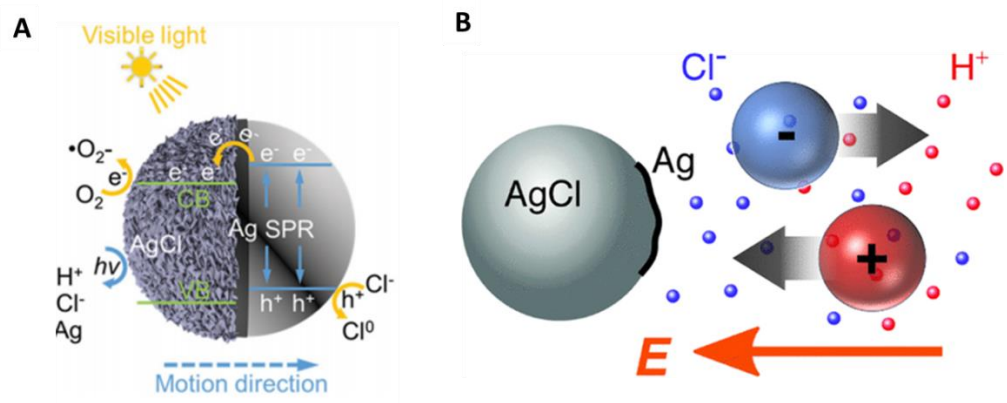

Figure 5. (A) Schematic illustration of the photodecomposition reaction of the AgCl cap triggered by blue light illumination[36]. (B) Schematic representation of the self-diffusiophoresis mechanism near an AgCl particle[37].

Since the Janus micromotors are generating a chemical gradient, passive particles present in solution can interact with it. Positive charged particles would be pumped and electrostatically attached to the Janus micromotors, while negative charged particles would move away from the Janus micromotors creating an exclusion zone around them[28,29]. The exclusion behavior is illustrated in Figure 6. The forces generated around the Janus particles remain active even when they are fixed at the substrate.

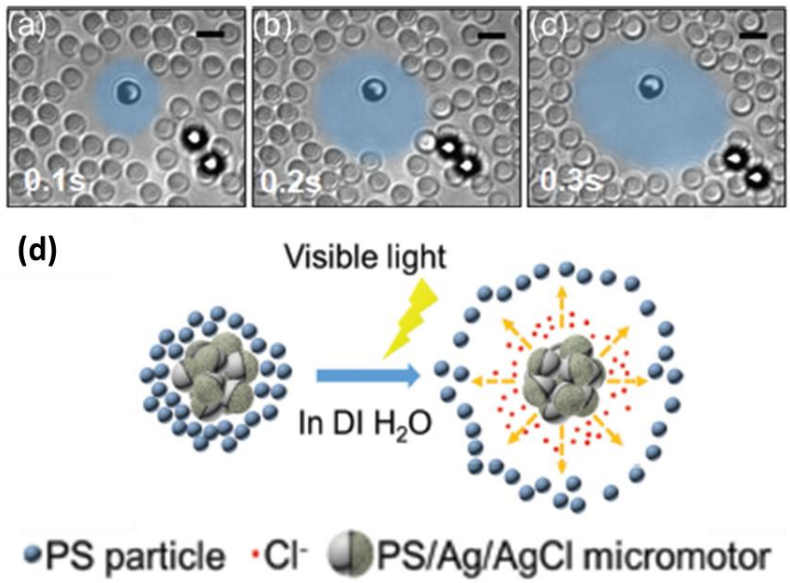

Figure 6. Exclusion behavior of pasive silica particles around Janus PS/Ag/AgCl. Interaction of a single Janus particle fixed at the substrate with passive silica particles at (a) 0.1 s, (b) 0.2 s, and (c) 0.3 s. (d) Schematic illustration of the blue-light induced exclusion process between a cluster of Janus PS/Ag/AgCl and passive silica particles. Figure adapted from Wang et al.[29]

Overall, these interesting phenomena make the Janus PS/Ag/AgCl micromotors a suitable non-biological model to study cell signaling and collective behavior[28]. Furthermore, the coordinated motion makes them attractive for applications such as transport and cargo delivery, chemical sensing, biomedical and environmental remediation[29].

1.5 Aim

The increasing demand to develop more accurate diagnostic tests that can be employed even in the most remote parts of the world where there are no specialized laboratories has led to the integration of different technologies that can aid to fulfill these requirements. The aim of this master thesis is to contribute to overcome this challenge by introducing the preliminary work of a LOC system for POC testing.

In summary, the main purpose of this work is to perform an indirect agglutination assay in micrometer sized wells using Janus micromotors to enhance the interaction between functionalized particles and antibodies. This concept is illustrated in Figure 7.

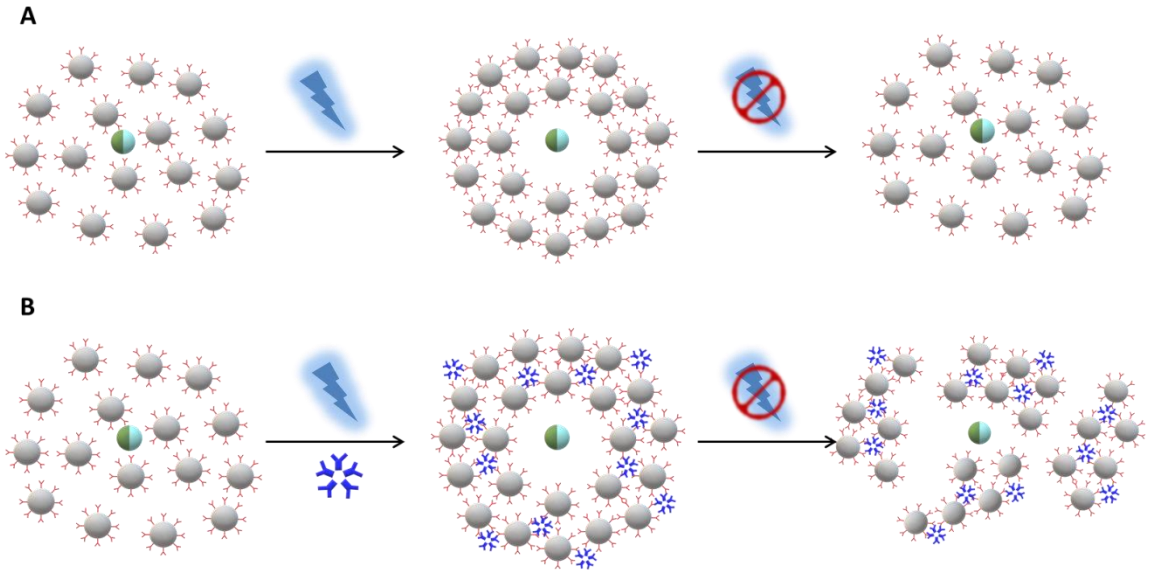

Figure 7. Conceptual schematic representation of the microswimmer-activated agglutination assay. (A) Janus microswimmer promotes the exclusion of functionalized particles when it is illuminated with blue light. When the light is turned off, the exclusion disappears. (B) When IgM antibody is present, the Janus microswimmer would promote the interaction of the functionalized particles and the antibody, allowing them to agglutinate. When the light is turned off, the particles will remain in clusters.

The first part of this work involves the fabrication and characterization of the main elements needed to perform the proposed assay: microwell chips as reaction chambers, Janus PS/Ag/AgCl micromotors as agglutination promoters, and functionalized particles for the agglutination assay. The second part of the thesis studies the interaction of the Janus micromotors with different particles, and the third and final section addresses the implementation of the indirect agglutination assay.

It is believed that systems similar to the proposed one can reduce assay time and detect lower analyte concentrations. In addition, this type of systems could be integrated with, for example, impedimetric-based sensors that would be able to monitor the agglutination of the particles with respect to different analyte concentrations and, as a result, they would be able to give more accurate and quantitative results.

The work realized during this master thesis provides the first steps towards the implementation of a fully-integrated lab-on-a-chip agglutination assay for point-of-care testing.

2. Materials and Methods

2.1 Microwell fabrication

Following a common UV-photolithography process, 40 micrometer-sized wells were fabricated to perform the proposed agglutination assay. Starting from cleaned glass slides, a thin layer of Ti-Prime (MicroChemicals GmbH) was deposited at 4000 rpm for 50 s and further baked at 120°C for 2 min to assure adhesion of the glass substrate and the subsequent coating. A 15 µm thick SU-8 (MicroChem) layer was then deposited with a spin coater RC 8 (Karl Suss) followed by a pre-baking step at 95°C for 6 min. The SU-8 coated substrate was then exposed to UV light (SUSS MicroTec) for 7.5 s and post-baked for 12 min at 95°C. To obtain the final structure the SU-8 was developed in mrDev600 (micro resist technology GmbH) for 4 min using ultrasonic bath, rinsed with isopropanol and hard-baked at 180°C for 1 h. These steps are summarized in Figure 8.

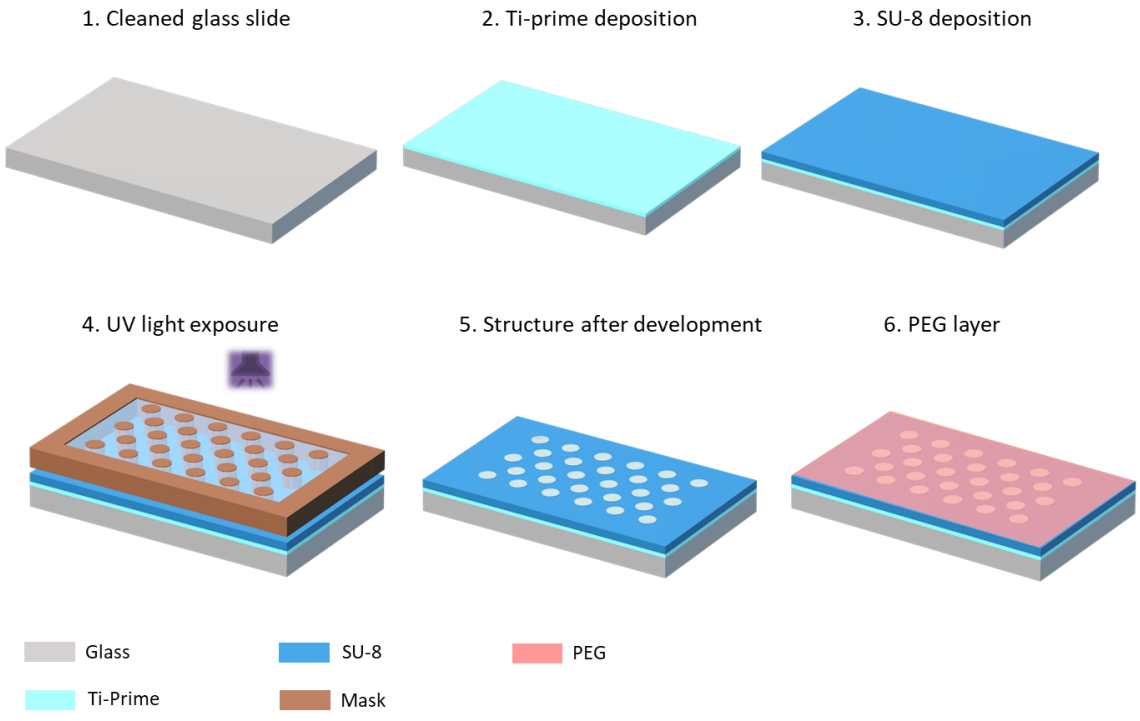

Figure 8. Schematic representation of the UV-photolitography process followed for the fabrication of microwells (40 µm in diameter). (1) The process started with a cleaned was slide. (2) Ti-prime was deposited and baked for 2 min. (3) SU-8 was deposited and pre-baked. (4) The resist was exposed to UV-light using a mask with the appropriate design to obtain 40 µm wells. SU-8 was post-baked, developed and rinse. (5) Final structure obtained after being hard-baked. (6) Microwells with PEG layer.

The agglutination assay involves the use of proteins which are known to have nonspecific absorption to hydrophobic substrates such as SU-8 and glass[38,39]. To prevent this, a poly(ethylene glycol) (PEG) layer was formed over the fabricated microwells. The substrates containing the microwells were treated with atmospheric oxygen plasma (Zepto system, Diener electronic GmbH) at 100 W for 1 min to expose OH^- groups on the surface. Then, the substrates were placed in a 1% PEG (Sigma-Aldrich, mol wt. 8000) solution for 10 min and dried using N_2 gun. To remove any remaining solvent, the substrates were baked at 100°C for 10 min.

2.2 Microswimmers fabrication

The fabrication of light-driven Janus PS/Ag/AgCl microswimmers begins with the formation of a monolayer of 2 μm PS particles (Sigma-Aldrich). This monolayer was achieved by drop casting the PS particles in ethanol suspension (25 mg/mL) over water covered glass slides previously processed by atmospheric oxygen plasma. The monolayer forms at the air-water interface and it was transferred to the glass slides (that are located at the bottom) by carefully removing the water from the edges using a pipette. Once the solvent was removed and the glass slides were air dried, the monolayer of PS particles was located on the surface of the glass slides. A 60 nm Ag layer was then deposit on the upper side of the monolayer by electron beam deposition. The Ag covered PS particles were suspended in DI water. To convert the Ag into AgCl, the Janus particles were dispersed in a 0.02 M $FeCl_3$ (Sigma-Aldrich) solution and an excess of 50 mM PVP (Sigma-Aldrich) solution was added. This reaction was performed in dark environment at room temperature for 1 h with constant stirring. When reaction was finished, the particles were washed five times and suspended in deionized (DI) water for further use. The schematic representation of the fabrication process of the Janus microswimmers is depicted in Figure 9.

2.3 Functionalization of particles

To perform an agglutination assay, micrometer-sized passive particles have to be functionalized with the appropriate antigen or antibody. For this thesis, 1.01 μm SiO_2-NH_2 particles (Bangs Laboratories, Inc.) and 2.12 μm SiO_2-NH_2 particles (microParticles GmbH) were functionalized with goat anti-human IgM secondary antibody (ThermoFischer) following the protocol for covalent coupling of Bangs

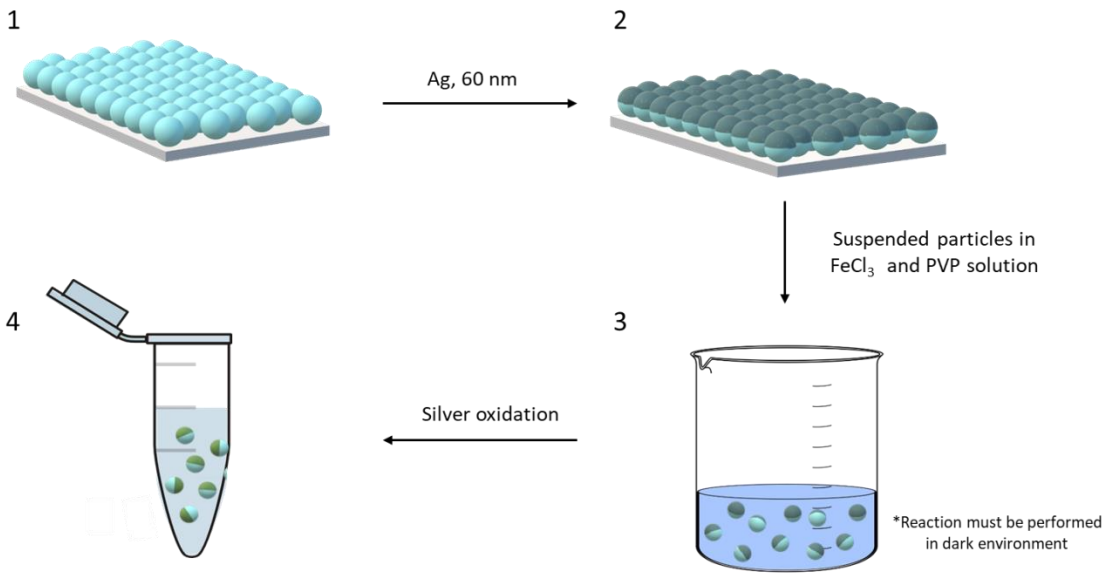

Figure 9. Schematic representation of the fabrication process of Janus particles. (1) A PS monolayer is formed over a glass slide. (2) A 60 nm thick layer of Ag is deposited on the upper side of the monolayer creating a half coating. (3) The particles are detached from the substrate and suspended in a solution of $FeCl_3$ and PVP to convert the Ag into AgCl. This reaction was performed in dark environment. (4) After Ag oxidation, particles are suspended in DI water and store in dark environment until used.

Laboratories[40]. The amount of secondary antibody needed to saturate the surface of the particles was estimated using the following equation:

$$S = (6/\rho Sd)(C) \qquad (2)$$

where S is the amount of antibody required for surface saturation, ρS is the density of the particle, d is the mean diameter of the particle and C is the capacity of the particle surface for a given antibody[40]. The value of C used to calculate S was 2.5 mg/m^2 [41].

The process started with washing 3.3 mg of 1.01 µm SiO_2-NH_2 particles and 7.14 mg of 2.12 µm SiO_2-NH_2 particles 2 times in 10 ml wash buffer (PBS, pH 7.4, Sigma-Aldrich). After second wash the particles were suspended in 10 ml of glutaraldehyde (Sigma-Aldrich) solution (glutaraldehyde dissolved in wash buffer to 10% final concentration) for 2 h at room temperature with constant stirring. After 2 h, the particles were washed 2 times and further suspended in 5 ml of wash buffer. The 5 ml particle suspension was combined with 0.005 mg of goat anti-human IgM secondary antibody previously diluted in 5 ml of wash buffer and allowed to react at room temperature for 4 h with continuous mixing. Once the reaction was finished, the

particles were washed 2 times (supernatant should be store to verify the functionalization) and suspended in quenching solution (35 mM glycine, 1% w/v BSA, Sigma-Aldrich) for 30 min with gentle mixing. Finally, the particles were washed 2 times, suspend in storage buffer (PBS with 0.01% w/v BSA) and store at 4°C until used.

2.4 Characterization of particles

2.4.1 Scanning electron microscope

The scanning electron microscope (SEM) allows observation of materials within the nanometer and micrometer scale. With this instrument you can obtain 3-dimensional images of the surface of materials[42]. To verify the fabrication of the Janus Ps/Ag/AgCl particles, SEM micrographs were acquired at 10 kV with a XL30 (Philips/FEI) SEM.

2.4.2 UV-vis spectroscopy

UV-vis spectroscopy is a quantitative technique that is based on the interaction of light with matter. This technique is widely employed to calculate the concentration of proteins in solution by measuring the absorbance at 280 nm and using Lambert-Beer law[43]. At his particular wavelength, the aromatic amino acids tyrosine and tryptophan exhibit a strong light absorption; as a consequence, the absorption of a protein at 280 nm is proportional to the content of these amino acids[44].

UV-vis spectroscopy was used to verify the binding of goat anti-human IgM secondary antibodies attached to the surface of the 1.01 and 2.12 μm SiO_2-NH_2 particles. The amount of free protein in solution after the reaction was determined by a standard curve using a UV-6300PC double beam spectrophotometer (VWR). The absorbance of the supernatants of both sizes of particles was measured and the concentration was calculated using a linear regression equation.

2.4.3 Zeta potential

The movement of colloids has a direct dependency on the value of the zeta potentials of the particles involved and the walls surrounding them[28,45]. The zeta potential

characterizes the electrical double layer of a solid surface and its value can be used to discuss the interactions between solid-solid and solid liquid interfaces[46,47].

To understand how the particles used in this work were moving and interacting with each other, zeta potential measurements were performed using Zetazizer Nano ZSP (Malvern Panalytical) with a 10 mW red laser (632.8 nm).

2.4.4 Optical microscopy

Optical microscopy allows us to observe in the micrometer scale, and with the addition of digital imaging, we are capable of acquiring not only single images, but also to record interesting processes[48].

To visualize the effect of the Janus particles on different particles (passive and functionalized) and the agglutination of the functionalized particles when the agglutinating agent was added to solution, an inverted Axiovert 200 M microscope (Carl Zeiss) integrated with a 5120 (Cascade) video camera was used.

The videos were recorded at 14 fps using two types of light illuminations: green light for reference measurements and blue light to generate the photodecomposition of AgCl since the plasmonic Ag/AgCl cap of the Janus particles enables them to absorb at this wavelength. The green light was obtained from the microscope halogen lamp (12V, 100 W) and filter sets in green and yellow color. The blue light was provided by an external fluorescent lamp HBO103 (Carls Zeiss). The images and videos were analyzed using the software Fiji[49].

2.5 Motion Experiments

Two experiments were performed to visualize the effect of the chemical gradient around the Janus particle and different particles (passive and functionalized): exclusion time and on/off light cycles.

Janus particles were fixed at the bottom of the fabricated microwells and subsequently 5 µl of particles (passive or functionalized) were added. For the exclusion time experiment, the microwells containing the Janus particles and the passive or

functionalized particles were illuminated with blue light for 2 min. For the on/off light cycles experiment, the microwells containing the Janus particles and the passive or functionalized particles were illuminated in an alternating way for 10 s with blue light and 30 s without blue light for 3 min.

2.6 Agglutination assay

The agglutination assay was performed using two different substrates: microscope glass slides with a PEG layer and the fabricated microwells. 5 µl of functionalized particles (1.01 µm and 2.12 µm) was deposited over the substrate and subsequently 5 µl of Human IgM (Sigma-Aldrich) with a concentration of 500 ng/ml were used as agglutinating agent. Images were taken just after adding the Human IgM and as the experiment progressed.

To verify the agglutination, a negative control for each size of functionalized particles was realized by depositing 5 µl of functionalized particles over both substrates without the addition of the Human IgM. Images were taken just after adding the functionalized particles and as the experiment progressed.

Agglutination assay was also performed using the Janus particles that were fixed at the bottom of the microwells. The experiments were realized following the methodology of section 2.5, the only difference was the addition of Human IgM as agglutination agent.

2.7 Effect of PBS

2.7.1 Janus particles

Janus particles were suspended in different PBS concentrations (50, 5, and 0.5 mM) and deposited inside the microwells to study the effect of PBS on their motion. The particles were illuminated with blue light for 30 s and their trajectories were tracked using the software Fiji. The motion in PBS was compared to the motion of Janus particles suspended in DI water.

2.7.2 Agglutination assay

To verify the binding ability of the antibodies at low PBS concentrations, an agglutination assay was performed over a PEG-covered glass slide using 5 µl of 2 µm SiO_2–NH_2-Ab particles and 5 µl of Human IgM.

2.7.3 Exclusion of functionalized particles

To analyze the interaction of Janus and 2 µm SiO_2–NH_2-Ab particles at low PBS concentration, Janus particles were fixed at the bottom of the microwells and subsequently 5 µl of 2 µm SiO_2–NH_2-Ab suspended in 0.5 mM PBS concentration were added. The particles were illuminated with blue light for 30 s.

3. Results and Discussion

3.1 Microwell chip with integrated Janus particles

An optical microscope image of one of the fabricated microwellchips is shown in Figure 10A. The size of the microwells was elected so that it was possible to have a clear visualization of the Janus particles and the microwell at the same time. Since the Janus particles show active motion when illuminated with blue light, their trajectories do not remain in the same observation plane during the experiments. As a result, it is difficult to have a clear perspective of the influence of the flows produced by the photocatalytic reaction at the surface of the Janus particles on passive and functionalized particles. To overcome this situation, Janus particles were fixed at the bottom of the fabricated microwells as shown in Figure 10B.

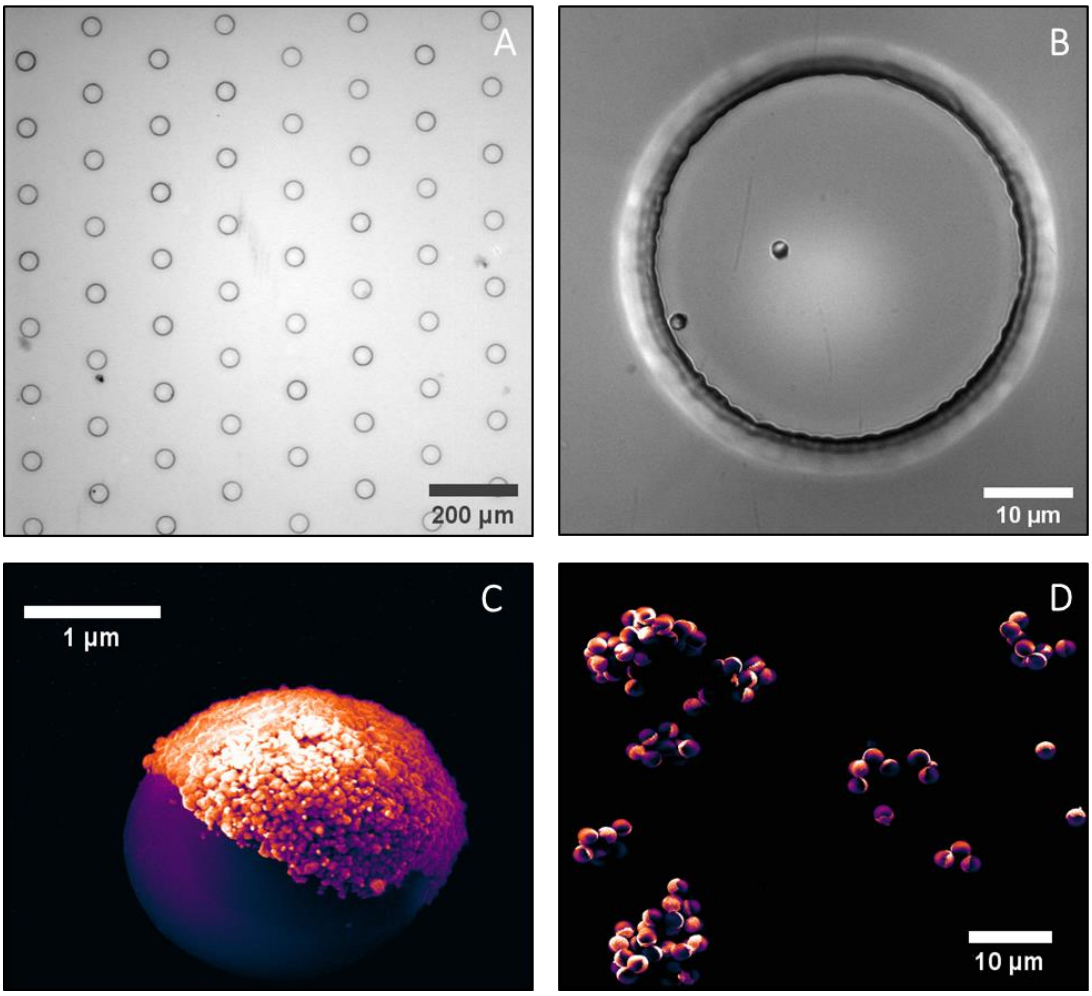

Figure 10. (A) Microwell chip. (B) Two Janus particles fixed at the bottom of a microwell. SEM images of one Janus particle (C) and various assemblies of Janus particles (D).

The presence of the Ag/AgCl cap of the fabricated Janus particles can be observed in the SEM images shown in Figure 10C-D. Apart from the single Janus particles, different assemblies of particles are visible. This is a consequence of the hydrophobic metal cap which causes the interaction between Janus particles in solution[29].

3.2 Characterization of particles

3.2.1 UV-vis spectroscopy

To verify the functionalization of the SiO_2-NH2 particles, the absorbance of goat anti-human IgM was measured at known concentrations to obtain the standard curve shown in Figure 11. With a linear regression analysis Equation 3 was obtained:

$$y = -0.0034 + 4.4542\,x \tag{3}$$

where y-axis designates the absorbance in A.U. and x-axis designates the goat anti-human IgM concentration in mg/ml.

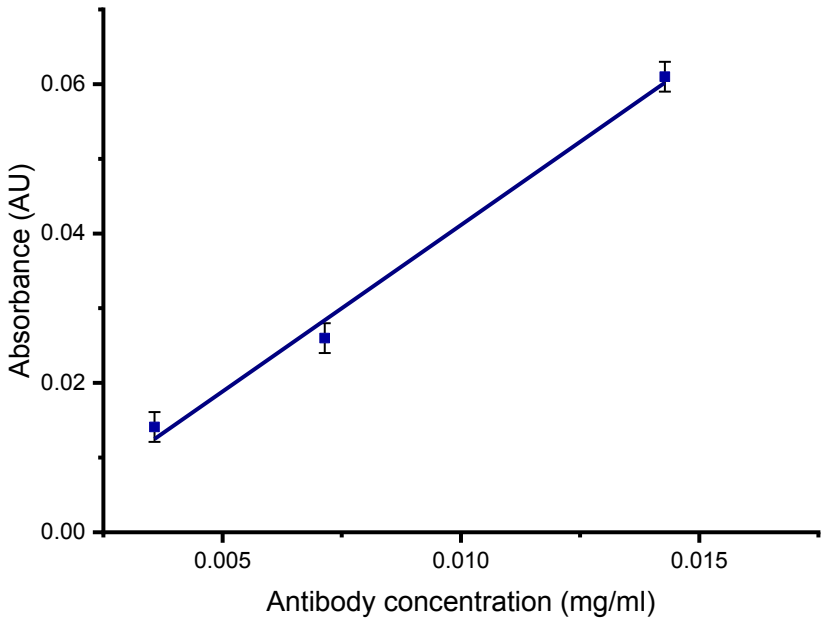

Figure 11. Standard curve for goat anti-human IgM.

With this analysis, it was possible to estimate the concentration of goat anti-human IgM in solution after the functionalization. This result shows the amount of goat anti-human IgM that was not covalently attached to the particles and since the initial concentration of antibody is known, the amount of antibody retained by the particles can be calculated. These results are reported in Table 1.

Table 1. Absorbance of supernatants at 280 nm, calculated concentration of goat anti-human IgM remaining in solution, amount of goat anti-human IgM covalently attached to the particles and amount of particles used for functionalization.

Sample	Absorbance of supernatant (A.U.)	Concentration goat anti-human IgM in supernatant (mg/ml)	Goat anti-human IgM attached to the particles (mg)	Weight of particles (mg)
1 μm SiO_2 –NH_2	0.0036	0.0016	0.0034	3.3
2 μm SiO_2 –NH_2	0.0033	0.0015	0.0035	7.14

Equation 2 suggests that the amount of secondary antibody needed to achieve surface saturation of 1 g of 1 μm and 2 μm SiO_2 –NH_2 particles was 7.5 mg and 3.5 mg respectively. It is recommended to use up to 10 times of the amount of secondary antibody that is necessary to obtain a monolayer when finding the optimal concentration for the functionalization since the coupling efficiency for different particles might vary. Particle composition, surface groups, surface charge density and hydrophilicity have an effect on the proximity of the antibody with the surface groups of the particle so that covalent coupling can be achieved.

For the functionalization, the initial concentration of goat anti-human IgM was 0.0050 mg/ml for both sizes of SiO_2 –NH_2 particles and 3.3 mg of 1 μm SiO_2 –NH_2 and 7.14 mg 2 μm SiO_2 –NH_2 particles were used so that the amount of secondary antibody was 2 times the amount needed to obtain a monolayer. As a result, it was expected that after the functionalization the amount of secondary antibody remaining in solution was the same for both sizes of particles, that is, half of the initial concentration. As it is shown in Table 1, the concentration of free secondary antibody in solution is approximately the same for both supernatants, but the concentration is less than expected. This can be due to the fact that for the calculation made using Equation 2, the value of C used was for bovine IgG with a molecular weight of 160 kD[41]. This value was experimentally obtained by Cantero et al. by adding different concentrations of antibody and measuring the amount of antibody that was absorbed by polystyrene tubes until saturation was reached[41]. Since the goat anti-human IgM

secondary antibody is an IgG with different characteristics from bovine IgG and it was attached to SiO_2–NH_2 particles that exhibit different properties compared to polystyrene tubes, the value of C is expected to differ from the one used. To have a better understanding of the capacity of the SiO_2–NH_2 particles for goat anti-human IgM secondary antibody, a similar experiment to the one performed by Cantero et al. should be realized.

3.2.2 Zeta potential

The main objective of this work was to achieve the motion of functionalized particles by means of the fluids generated around Janus particles when these are illuminated with blue light. To understand the interactions between the particles and their surroundings, the zeta potential of each of the particles used for the experiments was measured and it is reported in Table 2.

When a particle with net charge is suspended in a medium, an electrical double layer would form around it. Due to the charge of the particle, opposite charged ions are adsorbed to the surface and these ions would further attract the corresponding counterions, thus covering the surface of the particle with an electrical double layer[50,51]. This means that the same particle with different surface groups would have a different electrical double layer, and since the zeta potential characterizes the electrical double layer, the value of the zeta potential can be seen as an indicator of the functionalization of the particles.

Table 2. Zeta potential values for the different particles involved in the experiments.

Sample	Zeta potential (mV)
1 µm SiO_2 –NH_2	59.2
2 µm SiO_2 –NH_2	68.03
1 µm SiO_2 –NH_2-Ab	-7.94
2 µm SiO_2 –NH_2-Ab	-7.10
2 µm SiO_2	-38.76
PS/Ag/AgCl	-27 ± 2.4[29]

As shown in Table 2, before functionalization, both sizes of particles had a positive zeta potential, 59.2 mV for 1 µm and 68.03 mV for 2 µm particles. After functionalization the particles changed their zeta potential to -7.94 mV for 1 µm and -7.10 mV for 2 µm. This change in the value of the zeta potential was expected since the surface of the particles no longer had the amino groups exposed, but the secondary antibodies, whose charge is depended on their amino acid sequence, content and the pH of the medium[52,53].

3.2.3 Agglutination assay in PEG-covered glass slides

The final verification of the functionalization of the SiO_2 –NH_2 particles was done by performing an agglutination assay using an IgM concentration of 500 ng/ml. The results of the agglutination assay (top row) and the negative control (bottom row) for both sizes of particles are shown in Figure 12.

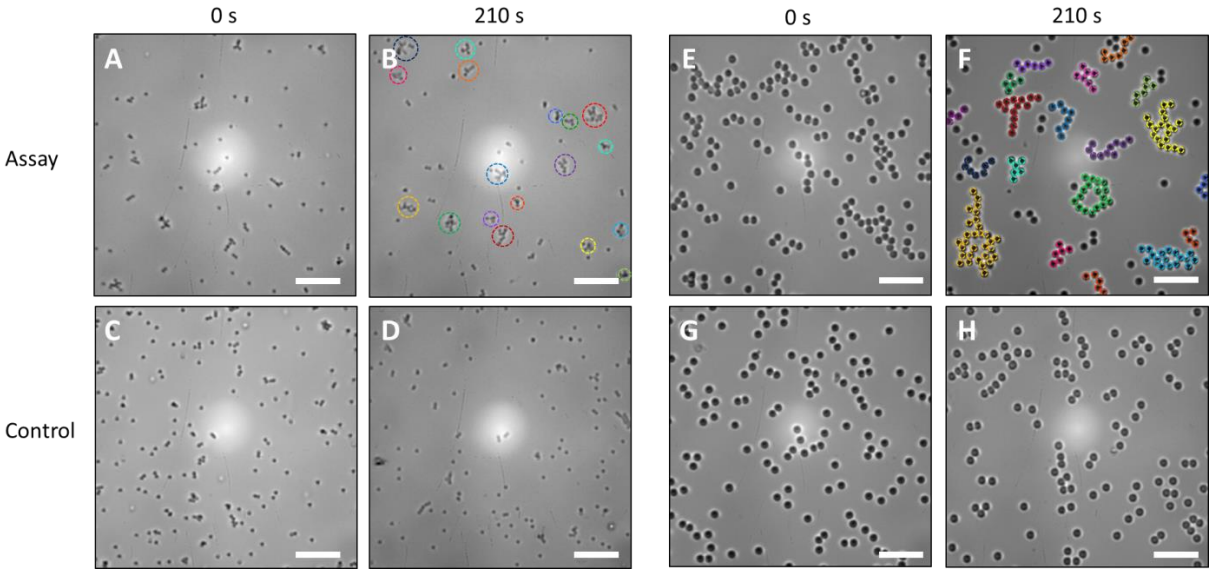

Figure 12. Agglutination assay performed over PEG-covered glass. Top row corresponds to the assay and bottom row to the negative control. A-D corresponds to 1 µm SiO_2–NH_2-Ab. E-H corresponds to 2 µm SiO_2 –NH_2-Ab particles. Scale bar is 10 µm.

The agglutination assay performed with 1 µm SiO_2–NH_2-Ab particles showed aggregation in clusters of size of approximate 10 particles, in addition some single particles were observed. The corresponding negative control exhibited small clusters of approximate 3 particles, while the majority of the particles were in a non-aggregated state. This result strongly indicates the functionalization of particles, as they aggregate in the presence of IgM, whereas the functionalized particles in the absence of IgM remained in a non-aggregated state.

The agglutination assay performed with 2 µm SiO_2–NH_2-Ab particles clearly showed that the particles aggregated in particular shapes, compared to the negative control that showed minimal association of particles. The linear and branched- like shapes of the clusters depicted in Figure 12F are similar to the resulting structures of a diffusion-limited aggregation (DLA) process[54]. This is applicable to cluster formation in which the particles have to diffuse to interact and agglomerate, such as the case of the agglutination assay[54]. A simulation of a structure formed by DLA process is shown in Figure 13.

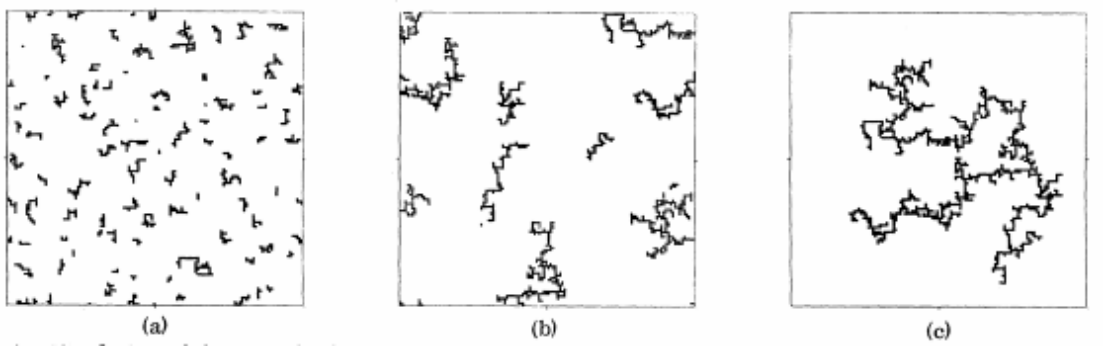

Figure 13. Simulation of the evolution of cluster formation of a growth model that describes the clustering of clusters of particles using 1024 particles. (a) Shows 86 clusters, (b) 8 clusters, and (c) 1 cluster[55].

3.3 Motion experiments

Motion experiments were realized to observe how passive SiO_2 particles, SiO_2–NH_2 particles, and functionalized SiO_2–NH_2-Ab particles respond to the flows generated around the Janus particles.

3.3.1 Exclusion time

Janus particles in presence of passive SiO_2 particles, SiO_2–NH_2 particles, and functionalized SiO_2–NH_2-Ab particles were illuminated continuously for 2 min with blue light. The response of each of the particles is shown in Figure 14.

Passive SiO_2 particles were excluded from the Janus particles (Figure 14A-C) while the SiO_2–NH_2 particles moved towards the Janus particles (Figure 14D-F for 1µm and Figure 14G-I). This opposite behavior can be explained by analyzing the diffusiophoretic interaction between the Janus particle and passive SiO_2 particles and

SiO_2–NH_2 particles. When Janus particles are illuminated with blue light, the AgCl located in the cap of the Janus particle will be photochemically decomposed as shown in Equation 1[28,56]. As explained by Wang et al., this reaction results in a radial flow of the produced ions from the surface of the Janus particle which will induce the self-propulsion of the Janus particles as well as the interaction with other particles present in the solution [29].

The produced ions during the photodecomposition of the AgCl cap have different diffusion rates which lead to a net electric field that is pointing towards the cap of the Janus particle (see Figure 5) [28,37]. This electric field will act phoretically on the particles and osmotically on any close electrical double layer[28]. As described by Ibele et al., particles with a positive zeta potential, such as the SiO_2–NH_2 particles used here, will be phoretically pumped towards the Janus particles and will be electrostatically attached to them since the zeta potential of the Janus particles is negative[28]. In contrast, particles with a negative zeta potential, such as the passive SiO_2 particles used, will be phoretically excluded from the Janus particles.

Figure 14B shows that the exclusion of passive SiO_2 particles around a Janus particle after 30 s of blue light illumination forms an exclusion zone of approximate 10 µm in diameter. After 2 min of constant blue light illumination the exclusion zone is no longer visible (Figure 14C). This is a consequence of the silver metal depositing back to the Janus particle cap[28,37]. This would cover the AgCl of the Janus cap not allowing the photodecomposition to continue.

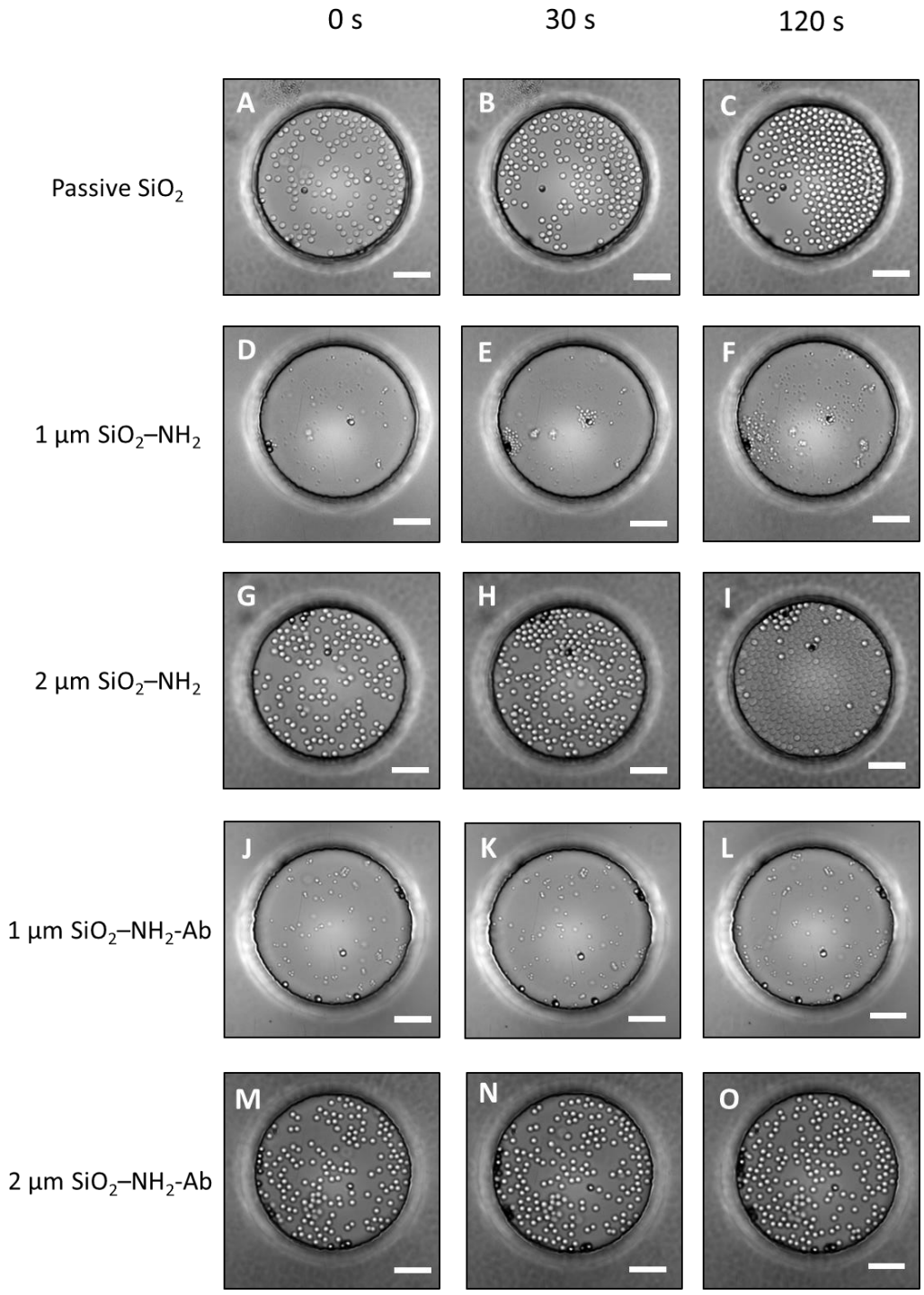

Figure 14. Exclusion time: the interaction of Janus particles and passive SiO_2 particles (A-C), 1 µm SiO_2–NH_2 (D-F), 2 µm SiO_2–NH_2 (G-H), 1 µm SiO_2–NH_2-Ab (J-L), 2 µm SiO_2–NH_2-Ab (M-O), while being exposed to blue light for 2 min. Scale bar is 10 µm.

The response of the functionalized particles to the flows produced by the Janus particles when illuminated with blue light are shown in Figure 14J-L for 1 µm SiO_2–NH_2-Ab and in Figure 14M-O for 2 µm SiO_2–NH_2-Ab. Since the zeta potential of both sizes of particles is negative, it was expected that they would be excluded from

the Janus particles; however, the functionalized particles do not show any noticeable response. This can be a consequence of the small value of the zeta potential and to the ions present in solution considering that the functionalized particles were dispersed in PBS solution. Both contributions will be briefly discussed in the following paragraphs.

The motion of particles as a result of an ionic gradient can be explained by the contribution of two effects: the electrophoretic force and the fluid flow generated by electro-osmosis[28,37,45]. Even though the Janus particles are fixed to the surface of the microwells, when illuminated with blue light flows and forces are generated around them as if they were suspended in solution[29]. The electric force that is generated around the Janus particles would exclude away particles with a negative zeta potential and attract particles with positive zeta potential[45]. However, the strength of the electric force directly depends on the value of the zeta potential of the particle, if the value of zeta potential is not sufficient, the electric force would not be enough to induce a motion on the particles. In this work, the functionalized particles have a zeta potential which is small compered to the values of zeta potential of particles that have shown either exclusion or attraction to the Janus particles.

As mentioned before, the electric field generated by the ionic gradient contributes to the motion of diffusiophoretic particles. When other ions are present in the bulk solution, they can screen the electric field. As a result, when increasing the concentration of ions in solution, the speed of diffusiophoretic particles decreases significantly[28]. This implies that the forces around the Janus particles are not enough to propel it, and this suggest that there will be no effect (exclusion or attraction) on other particles that are present in solution.

3.3.2 On/off light cycles

The results of the interaction of passive SiO_2 particles, 1 µm SiO_2–NH_2, 2 µm SiO_2–NH_2, 1 µm SiO_2–NH_2-Ab, 2 µm SiO_2–NH_2-Ab while being exposed to alternating blue light for 10 s on and 30 s off are shown in Figure 15. Each column represents a complete experiment of the type of particles mentioned at the top of the column.This experiment can be considered as a negative control since no IgM is added.

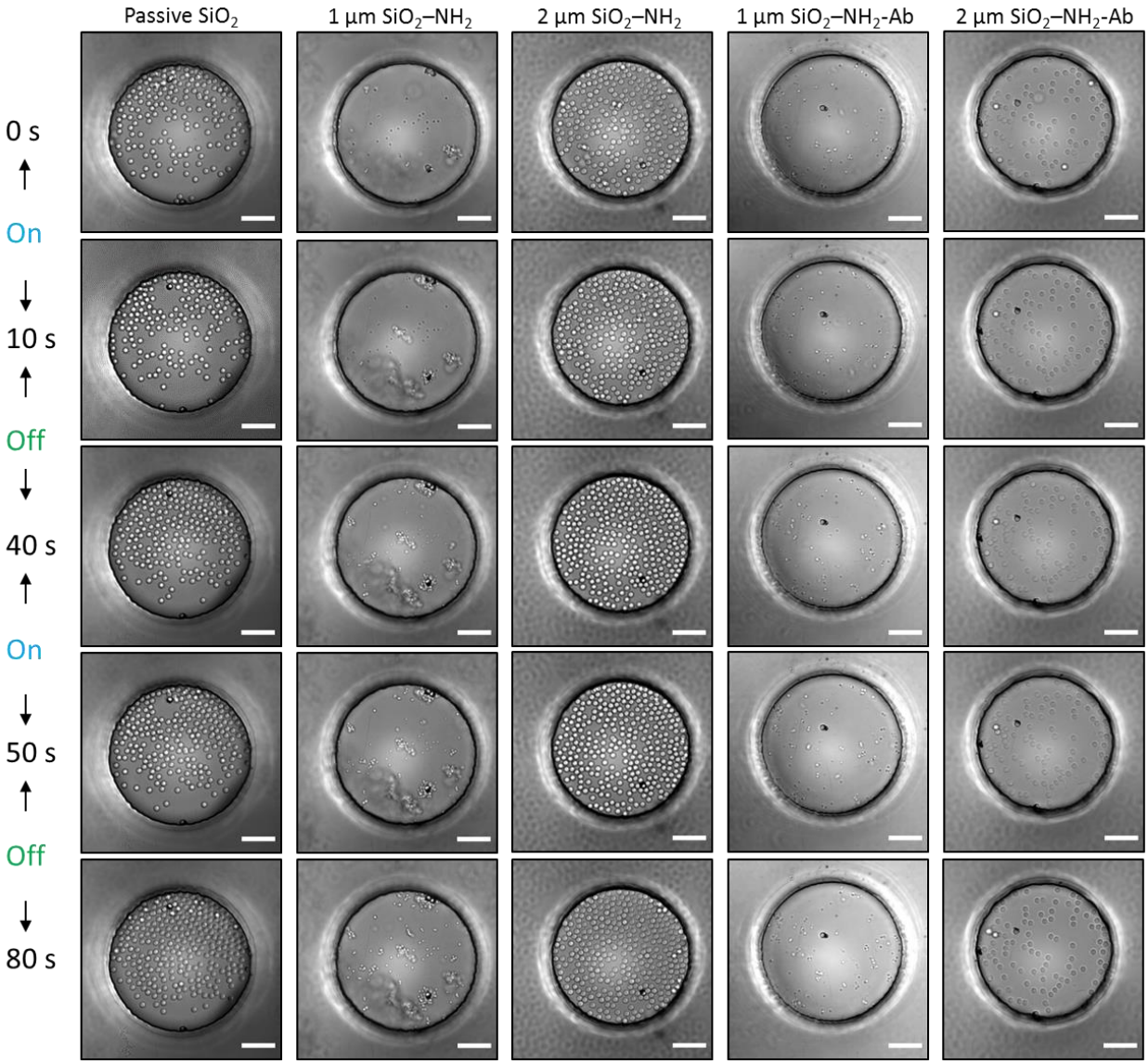

Figure 15. Interaction of Janus particles and passive SiO_2 particles (A), 1 µm SiO_2–NH_2 (B), 2 µm SiO_2–NH_2 (C), 1 µm SiO_2–NH_2-Ab (D), 2 µm SiO_2–NH_2-Ab (E), while being exposed to alternating blue light for 10 s on and 30 s off. Scale bar is 10 µm.

The aim of this thesis was to demonstrate the Janus particles could act as agglutination promoters considering that the flows produced around them promote the interaction (exclusion or attraction) of other particles present in solution. For that reason, it was expected that when IgM was present in solution the interaction between the particles would be irreversible. The purpose of the experiment of alternating light cycles was to have a clear visualization of the agglutination of particles. Without IgM it was expected that particles would exclude (or attract) the Janus particle when blue light is on and relax when the light is off (negative control), and with IgM it was

expected that particles would exclude (or attract) and remain in that state when the light is turned off.

The results of the negative control when passive SiO_2 particles are used clarly shows the concept explained in the previous paragraph. At time 0 s, passive SiO_2 particles are in close contact with the Janus particle. When blue light is on, the particles are excluded away from the cap. After 10 s of blue light illumination the particles relax and come around the Janus particle. When illuminated again, the particles are excluded and then relax back once the light is off. As explained before, silver metal produced during photodecomposition coats back into the cap blocking the AgCl available for reaction. As a result the size of the exclusion zone at time 50 s is slightly smaller than the size of the exclusion zone at 10 s.

From the results from section 3.3.1, it was expected to observe the same behaviour with SiO_2–NH_2 particles but with attraction of the particles to the Janus particles instead of being excluded. However, the electrostatic interaction between the Janus particles and the SiO_2–NH_2 particles was very strong, thus the particles were not able to relax (Figure 15B-C).

By virtue of the results reported in the previous section it was anticipated that the functionalized SiO_2–NH_2-Ab particles would not have any response during the light cycles. This can be confirmed in the columns D and E from Figure 15.

3.4 Agglutination assay

3.4.1 Assay performed in wells

Before executing the agglutination assays using Janus particles as agglutination promoters, agglutination assays without Janus particles were performed with both sizes of functionalized SiO_2–NH_2-Ab particles. The results are presented in Figure 16.

Both sizes of functionalized particles show agglutination compared to their respective controls. The sizes of the aggregates formed by 1 μm SiO2–NH2-Ab are comparable to those shown in Figure 12B. However, with respect to Figure 12F, the sizes of the

aggregates formed by 2 µm SiO2–NH2-Ab are smaller. This can be a result of the amount of particles that are inside the microwell. There are fewer particles inside the microwell that are available to interact than the amount of particles that are interacting in Figure 12E-F.

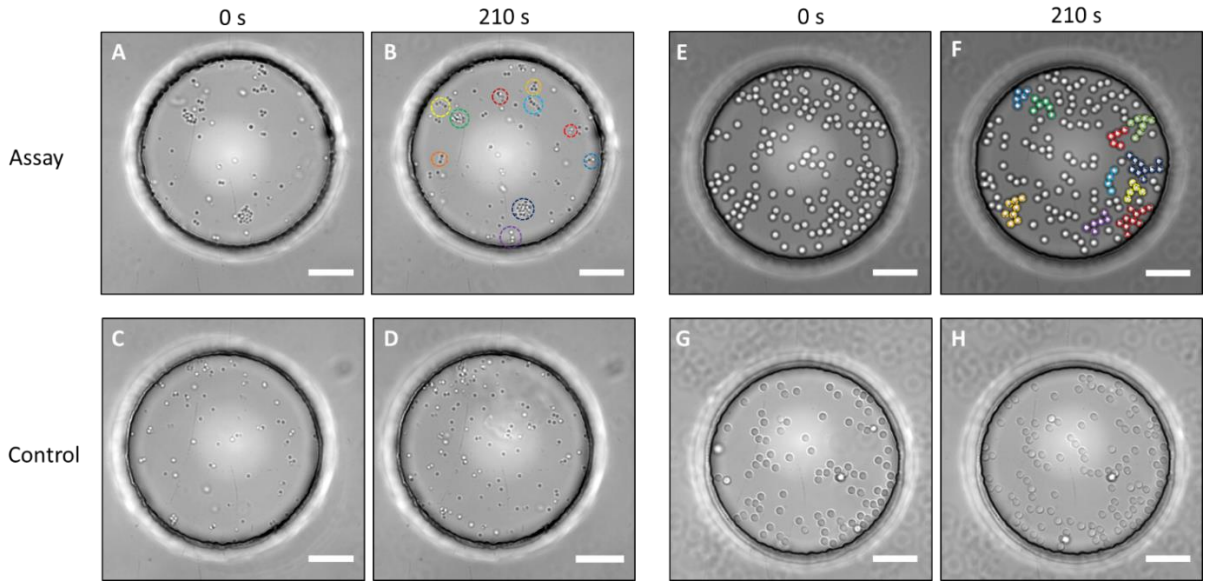

Figure 16. Agglutination assay performed microwells. Top row corresponds to the assay and bottom row to the negative control. A-D corresponds to 1 µm SiO2–NH2-Ab. E-H corresponds to 2 µm SiO2 – NH2-Ab particles. Scale bar is 10 µm.

3.4.2 Assay performed in wells with Janus particles

The results of these experiments were thought to probe that Janus particles could act as agglutination promoters during agglutination assays. However, as it has been previously discussed, the functionalized particles do not respond to the flows and forces produced around the Janus particle when illuminated with blue light. Therefore, it was expected that no interaction of the functionalized particles and the Janus particles would have happened. That can be confirmed in Figure 17B for 1 µm SiO2–NH2-Ab and in Figure 17F for 2 µm SiO2–NH2-Ab.

Despite that there was no visible interaction between the Janus particles and the functionalized particles agglutination was expected since IgM was present in solution. In Figure 17B for 1 µm SiO2–NH2-Ab and in Figure 17F for 2 µm SiO2–NH2-Ab, some agglutination of the functionalized particles is visible.

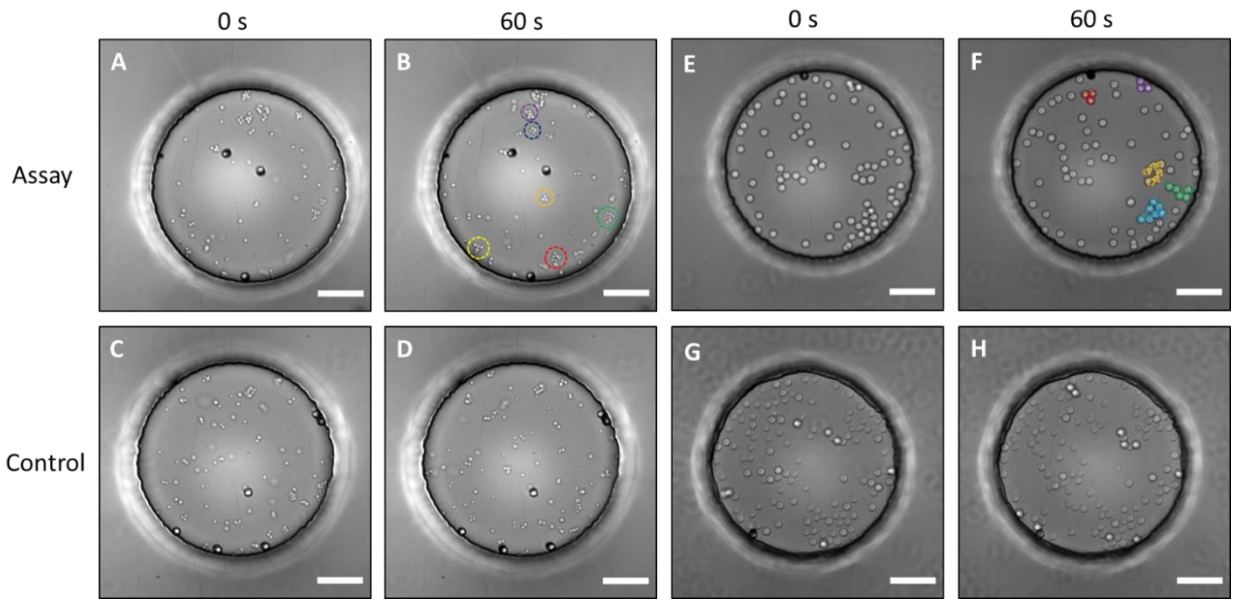

Figure 17. Agglutination assay performed microwells in presence of Janus particles. Top row corresponds to the assay and bottom row to the negative control. A-D corresponds to 1 µm SiO2–NH2-Ab. E-H corresponds to 2 µm SiO2 –NH2-Ab particles. Scale bar is 10 µm.

3.5 Effect of PBS concentration

3.5.1 Janus particles

As discussed in section 3.3.1, the extra ions provided by the functionalized particles suspended in PBS could affect the the propulsion of the Janus particles, and, as a result, no interaction between the Janus particles and functionalized particles was observed. However, antibodies (in this case goat anti-human IgM and human IgM) work under physiological conditions which requiere the use of PBS and a pH of 7.4. For that reason it is important that the Janus particle can generate flows around itself in physiological conditions.

The motion of the Janus particles was studied under different concentrations of PBS to observe how the speed changes compare to the motion of Janus particles in water. Figure 18 shows the results of the motion of the Janus particles being illuminated for 30 s. The tracking column displays the trajectory of the moving particles from time 0 s to 30 s.

At high concentrations of PBS (50 and 5 mM) the majority of the Janus particles are fixed at the substrate and the ones that move show only Brownian motion. At 0.05

mM concentration of PBS, Janus particles exhibit some displacement; however, the trajectory followed in DI water is considerable larger.

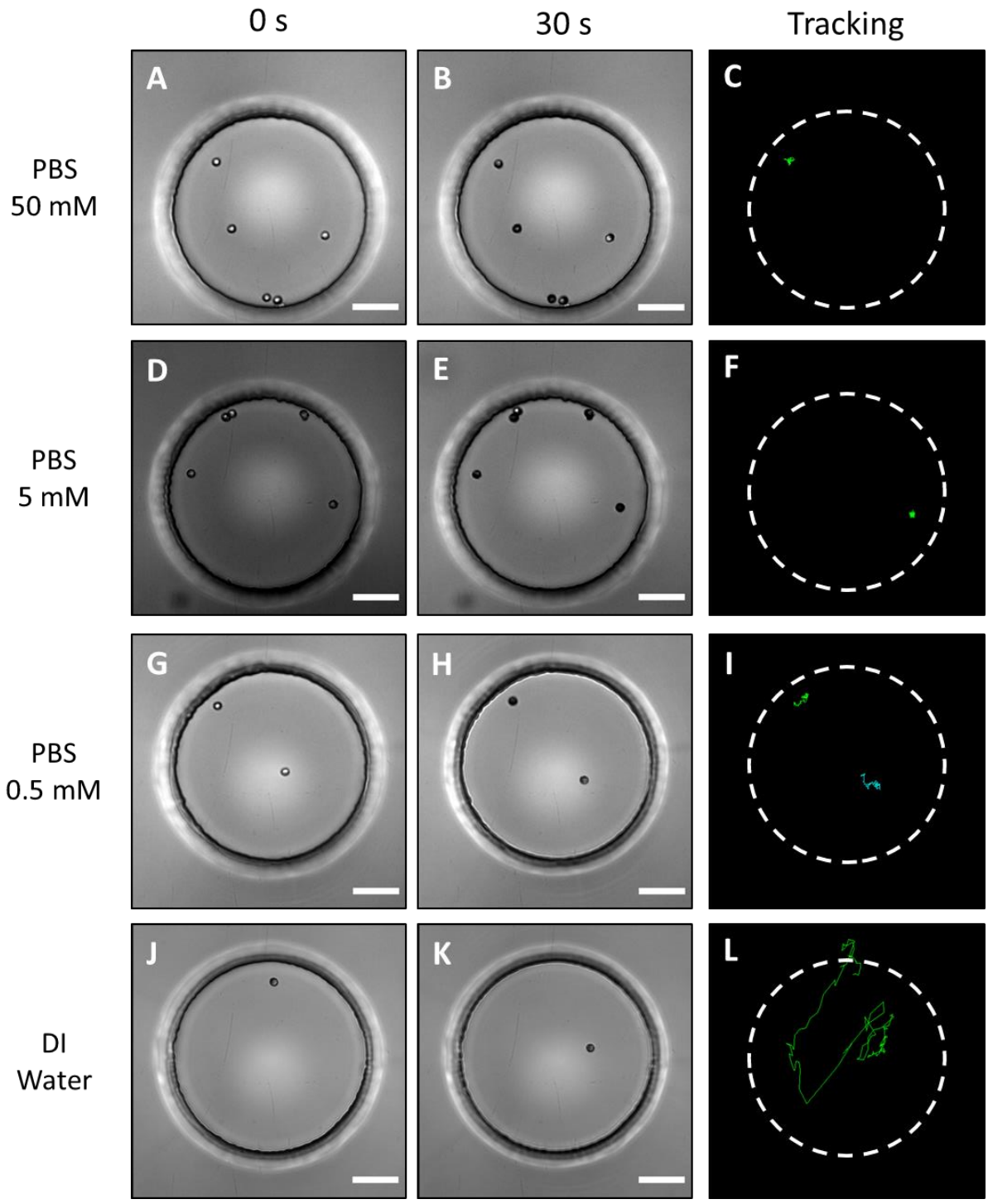

Figure 18. Effect of PBS on the motion of Janus particles. A-C Janus particles in 50 mM PBS. D-F Janus particles in 5 mM PBS. G-I Janus particles in 0.5 mM PBS. J-L Janus particles in DI water. Scale bar is 10 µm.

3.5.2 Agglutination assay

As it was previously mentioned, physiological conditions are required for the agglutination assay to work properly. On the other hand, to be able to use the Janus particles as agglutination promoters, the concentration of ions present in solution should be reduced. A compromise has to be reached to find the conditions in which the Janus particles could act as agglutination promoters and the antibodies maintain their functionalities.

As seen in the previous section the Janus particles exhibit some motion at 0.5 mM PBS concentration. For that reason, the agglutination of particles was tested with 2 µm SiO2 –NH2-Ab particles suspended in 0.5 mM PBS. The results of the agglutination assay are shown in Figure 19.

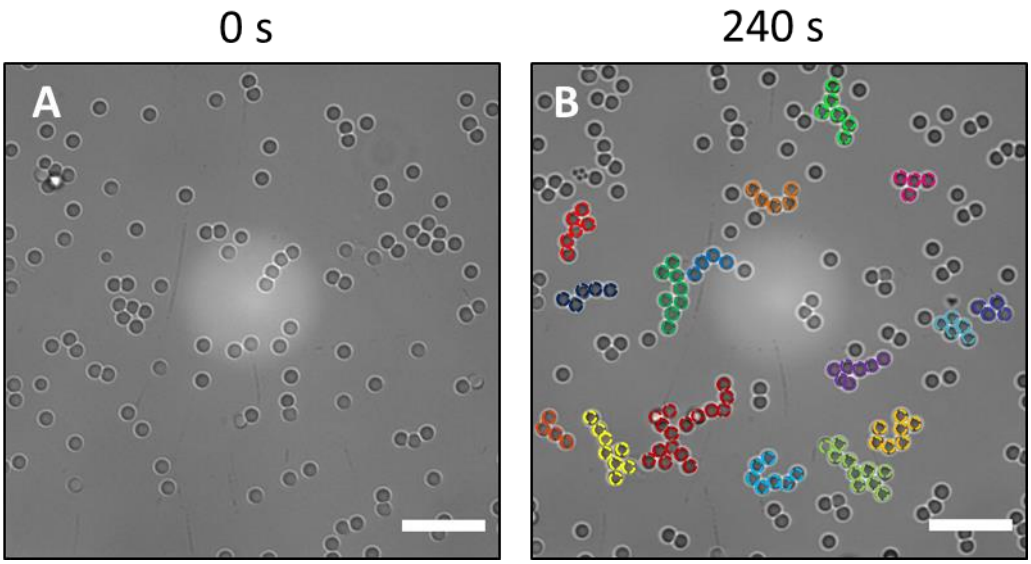

Figure 19. Agglutination assay using 2 µm SiO2 –NH2-Ab particles suspended in 0.5 mM PBS solution. Scale bar is 10 µm.

After 4 min, the agglutination of the particles is evident. This result, in addition to the results from the previous section, might suggest that 0.5 mM PBS is a suitable concentration for the test. Nevertheless, the IgM is supplied in PBS and since equal volumes of IgM and functionalized particles were used, the final concentration of PBS during this assay was higher than 0.5 mM.

Achieving a final concentration of 0.5 mM is not so straightforward considering that a dilution of IgM would imply less IgM available for interaction and, in the end, agglutination might not be visible. A careful methodology should be designed to obtain a suitable concentration of IgM for agglutination to happen and a suitable concentration of PBS so that both the Janus particles and the antibodies can work properly.

3.5.3 Exclusion of functionalized particles

To test if the concentration of PBS at which Janus particles exhibit some motion had an effect on the interaction with 2 μm SiO2 –NH2-Ab particles, a Janus particle was fixed at the bottom of a well and it was illuminated for 30 s with blue light in the presence of 2 μm SiO2 –NH2-Ab suspended in 0.5 mM PBS concentration.

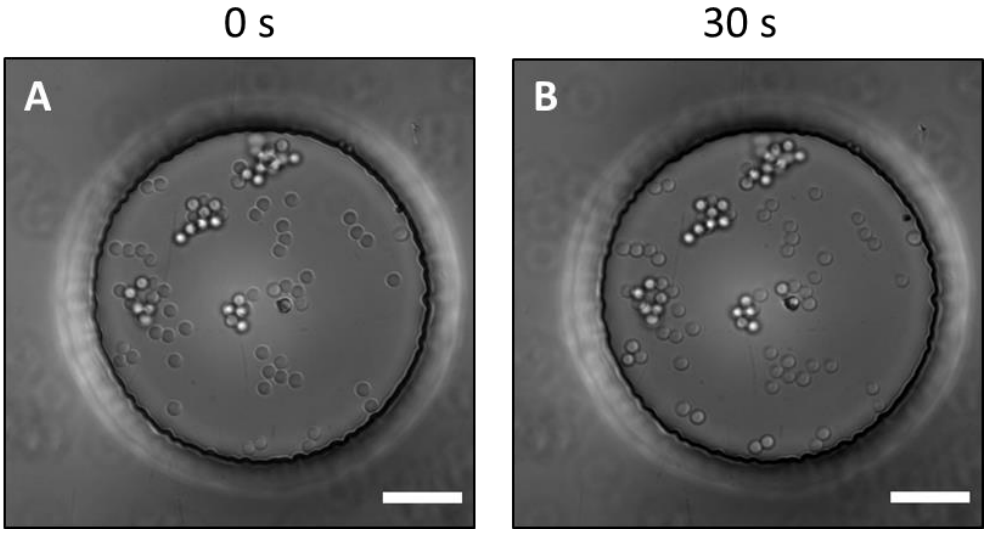

Figure 20. Interaction of Janus particle with 2 μm SiO2 –NH2-Ab particles suspended in 0.5 mM PBS solution.

As it can be seen in Figure 20, the Janus particle is not able to induce exclusion on the surrounding 2 μm SiO2 –NH2-Ab particles. This result together with results reported in section 3.5.1 give some important insight into the parameters that should be carefully modified to achieve the agglutination of functionalized particles promoted by the interaction with the Janus particles.

The results of the effect of the PBS concentration on the motion of the Janus particles showed that the motion is considerably affected by the ions present in solution. However, since even at low concentration of PBS the Janus particles were not able to

exclude the functionalized particles, this suggests that the value of the zeta potential is of great importance to achieve exclusion, as it was discussed in section 3.3.1.

The results obtained in this work provide the basis to achieve the agglutination of particles using Janus particles as agglutination promoters. It was found that the proper working conditions for the used antibodies and the Janus particles differed and as a result the interaction between the functionalized particles and the Janus particles was not visible. However, the key parameters affecting the interaction between the particles were discussed. Further experiments should be performed to find the conditions in which the concentration of IgM would be enough to produce agglutination, and the concentration of PBS is such that the Janus particles and the antibodies maintain their activities.

4. Conclusions

The interaction between Janus particles and passive SiO_2 particles, SiO_2–NH_2 particles, and functionalized SiO_2–NH_2-Ab particles was presented. Depending on the charge of the particles, attraction (for particles with positive zeta potential) or exclusion (particles with negative zeta potential) was observed. However, the magnitude of the zeta potential and the extra ions present in solution (ions from PBS solution) affected the fluid and forces produced around the Janus particles. As a result, particles suspended in PBS solution and with small zeta potential could not show any interaction with the Janus particles.

Motion experiments at different PBS concentrations showed that the movement of the Janus particles is considerably affected by the extra ions in solution. Only at 0.5 mM PBS concentration some motion vas observed, however it was minimal compare to motion of Janus particles in DI water. At this concentration of PBS, no exclusion is visible between the Janus and functionalized SiO_2–NH_2-Ab particles. This suggests that the value of zeta potential has a great influence on the exclusion of the functionalized particles. A more negative zeta potential of the functionalized particles should be achieved to have visible exclusion.

The results of the agglutination assays demonstrate that the particles were properly functionalized since in presence of IgM the particles form agglomerates. When the agglutination assay was performed in presence of the Janus particles, agglutination was visible but no exclusion of the functionalized particles was observed.

Agglutination assay was performed at 0.5 mM concentration of PBS since higher PBS concentrations greatly affect the flows and forces that are formed around the Janus particles. Agglutination of functionalized particles was visible at these conditions; however, the effective PBS concentration was higher due to the fact that the IgM is provided in PBS.

In summary, the proper working conditions for the antibodies and the Janus particles differed and, as a consequence, no interaction between the Janus and functionalized particles was visible. Taking into account the key parameters that affect the interaction between the particles (extra ions in solution and magnitude of the zeta potential), further experiments should be performed to find the conditions at which the concentration of PBS would allow the Janus particles and the antibodies to maintain their activities, and the concentration of IgM is enough to produce agglutination.

The work realized in the course of this master thesis provides the first steps towards the development of a lab-on-a-chip agglutination assay for point-of-care testing.

References

1. Naumov, L. B. Main problems of modern medicine in diagnostics and learning: ways of optimal solution. *Anadolu Kardiyol Derg* **1**, 166–178 (2001).
2. Kosack, C. S., Page, A.-L. & Klatser, P. R. Policy & practice A guide to aid the selection of diagnostic tests. *Bull World Heal. Organ* **95**, 639–645 (2017).
3. Organization, W. H. Laboratory and in vitro diagnostics. (2019). Available at: https://www.who.int/in-vitro-diagnostic/en/. (Accessed: 15th July 2019)
4. Leeflang, M. M. G. & Allerberger, F. How to: evaluate a diagnostic test. *Clin. Microbiol. Infect.* **25**, 54–59 (2019).
5. Commission, E. The In Vitro Diagnostic Medical Devices Directive (98/79/EC). *Off. J. Eur. Communities* 7.12 (1998).
6. Cheng, C.-M., Kuan, C.-M. & Chen, C. *In-vitro diagnostic devices: Introduction to current point-of-care diagnostic devices*. (2015). doi:10.1007/978-3-319-19737-1
7. Lee, G. C. *et al.* Development and evaluation of a rapid diagnostic test for Plasmodium falciparum, P. vivax, and mixed-species malaria antigens. *Am. J. Trop. Med. Hyg.* **85**, 989–993 (2011).
8. Cai, H. Y., Caswell, J. L. & Prescott, J. F. Nonculture Molecular Techniques for Diagnosis of Bacterial Disease in Animals: A Diagnostic Laboratory Perspective. *Vet. Pathol.* **51**, 341–350 (2014).
9. Kwok, S. *et al.* Identification of human immunodeficiency virus sequences by using in vitro enzymatic amplification and oligomer cleavage detection. *J. Virol.* **61**, 1690–4 (1987).
10. Saiki, R. K. *et al.* Enzymatic amplification of beta-globin genomic sequences and restriction site analysis for diagnosis of sickle cell anemia. 1985. *Biotechnology* **24**, 476–480 (1992).
11. O'Donnell, O. Access to health care in developing countries: breaking down demand side barriers. *Cad. Saude Publica* **23**, 2820–34 (2007).
12. Vashist, S. K. Point-of-care diagnostics: Recent advances and trends. *Biosensors* **7**, 10–13 (2017).

13. Koczula, K. M. & Gallotta, A. Lateral flow assays. *Essays Biochem.* **60**, 111–120 (2016).
14. Singer, J. M. & Plotz, C. M. The Latex Fixation Test: I. Application to the Serologic Diagnosis of Rheumatoid Arthritis. *American Journal of Medicine* **21**, 888–892 (1956).
15. Stavitsky, A. B. Agglutination. in *Encyclopedia of Immunology (Second Edition)* (ed. Delves, P. J.) 56–59 (Elsevier, 1998). doi:https://doi.org/10.1006/rwei.1999.0016
16. Austin, J. W. & Pagotto, F. J. MICROBIOLOGY | Detection of Foodborne Pathogens and their Toxins. in *Encyclopedia of Food Sciences and Nutrition (Second Edition)* (ed. Caballero, B.) 3886–3892 (Academic Press, 2003). doi:https://doi.org/10.1016/B0-12-227055-X/00774-4
17. Fronczek, C. F. & Yoon, J.-Y. Chapter 12 - Detection of Foodborne Pathogens Using Biosensors. in *Antimicrobial Food Packaging* (ed. Barros-Velázquez, J.) 153–166 (Academic Press, 2016). doi:https://doi.org/10.1016/B978-0-12-800723-5.00012-7
18. Lumen Learning. Agglutination Assays. Available at: https://courses.lumenlearning.com/suny-microbiology/chapter/agglutination-assays/. (Accessed: 1st April 2019)
19. Gupta, A. & Chaudhary, V. K. Whole-blood agglutination assay for on-site detection of human immunodeficiency virus infection. *J. Clin. Microbiol.* **41**, 2814–2821 (2003).
20. Branch, S. L. & Levett, P. N. Evaluation of four methods for detection of immunoglobulin M antibodies to dengue virus. *Clin. Diagn. Lab. Immunol.* **6**, 555–7 (1999).
21. Chew, D. J., DiBartola, S. P. & Schenck, P. A. Chapter 14 - Tumors of the Urinary System. in *Canine and Feline Nephrology and Urology (Second Edition)* (eds. Chew, D. J., DiBartola, S. P. & Schenck, P. A.) 434–464 (W.B. Saunders, 2011). doi:https://doi.org/10.1016/B978-0-7216-8178-8.10014-4
22. Lee, J. & Lee, S. H. Lab on a chip for in situ diagnosis: From blood to point of care. *Biomed. Eng. Lett.* **3**, 59–66 (2013).
23. Gupta, S., Kilpatrick, P. K., Melvin, E. & Velev, O. D. On-chip latex agglutination immunoassay readout by electrochemical impedance

spectroscopy. *Lab Chip* **12**, 4279–4286 (2012).

24. Mohammed, M. I., Haswell, S. & Gibson, I. Lab-on-a-chip or Chip-in-a-lab: Challenges of Commercialization Lost in Translation. *Procedia Technol.* **20**, 54–59 (2015).
25. Maria-Hormigos, R., Jurado-Sánchez, B. & Escarpa, A. Labs-on-a-chip meet self-propelled micromotors. *Lab Chip* **16**, 2397–2407 (2016).
26. Castillo-leon, J. *Lab-on-a-Chip Devices and Micro-Total Analysis Systems*. *Lab-on-a-Chip Devices and Micro-Total Analysis Systems* (2014). doi:10.1007/978-3-319-08687-3
27. García, M. *et al.* Micromotor-based lab-on-chip immunoassays. *Nanoscale* **5**, 1325–1331 (2013).
28. Ibele, M., Mallouk, T. E. & Sen, A. Schooling behavior of light-powered autonomous micromotors in water. *Angew. Chemie - Int. Ed.* **48**, 3308–3312 (2009).
29. Wang, X. *et al.* Visible Light Actuated Efficient Exclusion Between Plasmonic Ag/AgCl Micromotors and Passive Beads. *Small* **14**, (2018).
30. Guix, M., Mayorga-Martinez, C. C. & Merkoçi, A. Nano/Micromotors in (Bio)chemical science applications. *Chem. Rev.* **114**, 6285–6322 (2014).
31. P. Feynman, R. There is plenty of room at the bottom.pdf. *Eng. Sci.* **23**, 22–36 (1960).
32. Abdelmohsen, L. K. E. A., Peng, F., Tu, Y. & Wilson, D. A. Micro- and nano-motors for biomedical applications. *J. Mater. Chem. B* **2**, 2395–2408 (2014).
33. Gao, W. *et al.* Bioinspired helical microswimmers based on vascular plants. *Nano Lett.* **14**, 305–310 (2014).
34. Dong, R., Zhang, Q., Gao, W., Pei, A. & Ren, B. Highly efficient light-driven TiO2-Au Janus Micromotors. *ACS Nano* **10**, 839–844 (2016).
35. Sanchez, S., Soler, L. & Katuri, J. Chemically powered micro- and nanomotors. *Angew. Chemie - Int. Ed.* **54**, 1414–1444 (2015).
36. Wang, X. *et al.* High-Motility Visible Light-Driven Ag/AgCl Janus Micromotors. *Small* **14**, 1–11 (2018).
37. Zhou, C., Zhang, H. P., Tang, J. & Wang, W. Photochemically Powered AgCl Janus Micromotors as a Model System to Understand Ionic Self-Diffusiophoresis. *Langmuir* **34**, 3289–3295 (2018).

38. Tao, S. L., Popat, K. C., Norman, J. J. & Desai, T. A. Surface modification of SU-8 for enhanced biofunctionality and nonfouling properties. *Langmuir* **24**, 2631–2636 (2008).
39. Yang, Z., Galloway, J. A. & Yu, H. Protein interactions with poly(ethylene glycol) self-assembled monolayers on glass substrates: Diffusion and adsorption. *Langmuir* **15**, 8405–8411 (1999).
40. Bangs Laboratory. Covalent Coupling. (2013). doi:10.1007/3-540-29623-9_5754
41. Cantarero, L. A., Butler, J. E. & Osborne, J. W. The adsorptive characteristics of proteins for polystyrene and their significance in solid-phase immunoassays. *Anal. Biochem.* (1980). doi:10.1016/0003-2697(80)90473-X
42. Goldstein, J. I. *et al.* Introduction. in *Scanning Electron Microscopy and X-ray Microanalysis: Third Edition* 1–20 (Springer US, 2003). doi:10.1007/978-1-4615-0215-9_1
43. Pace, C. N., Vajdos, F., Fee, L., Grimsley, G. & Gray, T. How to measure and predict the molar absorption coefficient of a protein. *Protein Sci.* **4**, 2411–2423 (1995).
44. Note, T. NanoDrop One/One C and Multiskan Sky spectrophotometers.
45. Afshar Farniya, A., Esplandiu, M. J. & Bachtold, A. Sequential tasks performed by catalytic pumps for colloidal crystallization. *Langmuir* **30**, 11841–11845 (2014).
46. Anderson, J. Colloid Transport By Interfacial Forces. *Annu. Rev. Fluid Mech.* **21**, 61–99 (1989).
47. Hunter, R. J. *Zeta potential in colloid science: principles and applications (Vol.2)*. (Academic Press, 2013).
48. Davidson, M. W. & Abramowitz, M. Optical Microscopy. in *Encyclopedia of Imaging Science and Technology* (American Cancer Society, 2002). doi:10.1002/0471443395.img074
49. Schindelin, J. *et al.* Fiji: an open-source platform for biological-image analysis. *Nat. Methods* **9**, 676 (2012).
50. Park, S.-J. & Seo, M.-K. Chapter 1 - Intermolecular Force. in *Interface Science and Composites* (eds. Park, S.-J. & Seo, M.-K.) **18**, 1–57 (Elsevier, 2011).
51. Selvamani, V. Chapter 15 - Stability Studies on Nanomaterials Used in Drugs.

in *Characterization and Biology of Nanomaterials for Drug Delivery* (eds. Mohapatra, S. S., Ranjan, S., Dasgupta, N., Mishra, R. K. & Thomas, S.) 425–444 (Elsevier, 2019). doi:https://doi.org/10.1016/B978-0-12-814031-4.00015-5

52. Welch, N. G., Scoble, J. A., Muir, B. W. & Pigram, P. J. Orientation and characterization of immobilized antibodies for improved immunoassays (Review). *Biointerphases* **12**, 02D301 (2017).
53. Gitlin, I., Carbeck, J. D. & Whitesides, G. M. Why are proteins charged? Networks of charge-charge interactions in proteins measured by charge ladders and capillary electrophoresis. *Angew. Chemie - Int. Ed.* **45**, 3022–3060 (2006).
54. Witten, T. A. & Sander, L. M. Diffusion-limited aggregation. **27**, 5686–5697 (1983).
55. Kolb, M., Botet, R. & Jullien, R. Scaling of Kinetically Growing Clusters. *Phys. Rev. Lett.* 1123–1126 (1983).
56. Calzaferri, G. At the time he made the first photographs on paper: Did Henry Fox Talbot oxidize water to oxygen with sunlight? *Catal. Today* (1997). doi:10.1016/S0920-5861(97)82240-7

Declaration of Research Integrity and Good Scientific Practice

I hereby certify that I have authored this Master's Thesis entitled Microswimmer-activated agglutination assay and without undue assistance from third parties. No other than the resources and references indicated in this thesis have been used. I have marked both literal and accordingly adopted quotations as such. They were no additional persons involved in the spiritual preparation of the present thesis. I am aware that violations of this declaration may lead to subsequent withdrawal of the degree.

Dresden, Germany, August 5th, 2019.

Diana Isabel Sandoval Bojórquez